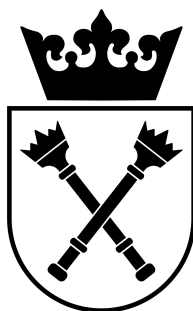


DOCTORAL DISSERTATION
PREPARED IN THE INSTITUTE OF PHYSICS
OF THE JAGIELLONIAN UNIVERSITY
SUBMITTED TO THE FACULTY OF PHYSICS,
ASTRONOMY AND APPLIED COMPUTER SCIENCE
OF THE JAGIELLONIAN UNIVERSITY



Hyperons @ HADES

Supervised by:
prof. dr hab. Piotr Salabura

Cracow, 2020

Wydział Fizyki, Astronomii i Informatyki Stosowanej
Uniwersytet Jagielloński

Oświadczenie

Ja niżej podpisany Krzysztof Nowakowski (nr indeksu: 1078309), doktorant Wydziału Fizyki Astronomii i Informatyki Stosowanej Uniwersytetu Jagiellońskiego, oświadczam, że przedłożona przeze mnie rozprawa doktorska pt. „Hyperons by HADES” jest oryginalna i przedstawia wyniki badań wykonanych przeze mnie osobiście, pod kierunkiem prof. dr. hab. Piotra Salabury. Pracę napisałem samodzielnie.

Oświadczam, że moja rozprawa doktorska została opracowana zgodnie z Ustawą o prawie autorskim i prawach pokrewnych z dnia 4 lutego 1994 r. (Dziennik Ustaw 1994 nr 24 poz. 83 wraz z późniejszymi zmianami).

Jestem świadom, że niezgodność niniejszego oświadczenia z prawdą ujawniona w dowolnym czasie, niezależnie od skutków prawnych wynikających z ww. ustawy, może spowodować unieważnienie stopnia nabytego na podstawie tej rozprawy.

Kraków, dnia

.....

Jakis mądry cytat

Autor „Zrodlo”

Ten sam cytat po angielsku

Autor, “Zrodlo”
Translation by Tlumacz

Abstract

sOME ABSTRACT

Streszczenie

Jakies streszczenie

Contents

Abstract	vii
1 Introduction	1
1.1 Hyperons	2
1.2 Form factors	2
1.3 Dalitz decays	4
2 The HADES detector	5
2.1 The HADES upgrades	5
3 Data analysis	7
3.1 Particles identification	7
3.2 Event selection	7
3.3 Reaction kinematics	8
3.4 The $\Lambda(1116)$ Reconstruction	8
3.5 The $\Lambda(1520)$ Reconstruction	8
3.6 The $\Lambda(1116)K^0$ reconstruction	8
3.7 results from p Nb experiment	8
4 Neural networks	9
4.1 Introduction into artificial neural networks	9
4.2 The ROC curve and the optimal classifier	9
4.3 The data-driven approach	9
4.4 Application for analysis	10
5 Simulations of a new experiment	13
5.1 An estimation of cross-sections	13
5.1.1 $\Lambda(1116)$ inclusive cross section	13
5.1.2 $\Sigma(1193)$ inclusive cross section	14
5.1.3 $\Lambda(1520)$, $\Lambda(1405)$ and $\Sigma(1385)$ production cross sections	14
5.1.4 $\Xi^-(1322)$	15
5.2 Decay branching ratios	16
5.3 Background channels selection	16
5.4 Simulations results	18
5.4.1 Particles identification	18
5.4.2 Hyperons Dalitz decays	18
5.4.3 Cascade decay	18

6 Conclusions	19
Appendices	21
Bibliography	21

Chapter 1

Introduction

The history of a particle physics is a fascinating journey towards the smallest, the most principle elements of the Universe. Starting from memorable Rutheford experiment in 1909 [1] up to Higgs boson discovery [2, 3], and misterous states X,Y,Z [ref] oserved at the begining of XXIth century. Throughout this entire journey there were many attemps to point out which particles are realy elementary, and classify them. Nowadays the knowledge about elementary particles is collected in theory colled the standart model (SM) which describes almost all known particles and interaction between them.

According to the Standard Model we can divide elementary particles into three groups: leptons and quarks, basic bricks of the universe and elementary bosons a force-carryng particles. In contrary to leptons bosons can not exist in the nature in free states. This phenomena called “a confiment” is still not fully understood. Nonetheless, as a result ot the confiment, we can observe quarks in bound states: mesons and baryons. Mesons have a baryonic number equal 0 and mostly consist of two quarks. However such an exotic object like glueball are also classyified as mesons. Baryons are characterized by barionic number different than 0. Commonly obsered in nature consist of three quarks, but rare objects, like pentaquark, also belong to baryons.

A quark model proposed by Gell-Mann and Zweig in 1964 [4, 5] describes well a hierarchy of ground barionic nad masonic states. However to discribe origin of paricles properties like mass or spin, and predict excited states, a theory of quarks dynamics is required. Interaction between quarks are dominated by the strong force. Its general description, given by quantum chromodynamisc is very demanding in sspecific problems. For high energy regime an asymptotic freedom allows to solve equation by a series expansion. For low energys two approaches are possible: a phenomenological models, or a lattice calculations. Especially a barionic spectrum is poorly known and requires further investigations.

1.1 Hyperons

Assuming that energy available in the system is below a J/ψ meson mass (3.1 GeV/c) we can acknowledge that all the matter is built of three types of quarks: up, down and strange. These quarks are treated in quark model as an irreducible representation of a SU3 symmetry group. The possible ground states for a three-quarks systems have been predicted by quark model and described by the baryon octet and the baryon decuplet. All baryons consisting a strange quark are called hyperons.

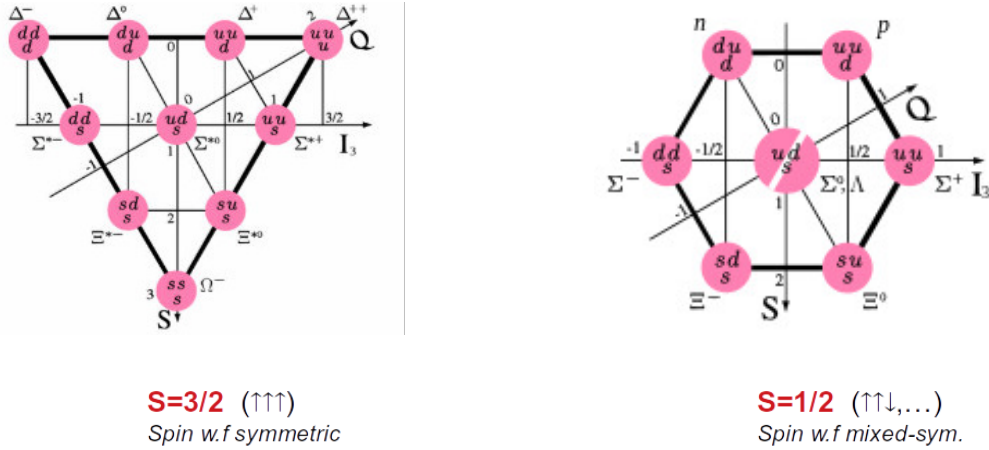


FIGURE 1.1: The eightfolds proposed by Gell-Mann and Ne'eman in 1961 to classify baryonic states. At a publication moment they classify all known baryons except the Ω^- . Its discovery in 1964 [6] was a great success of the quark model.

The quark model is very successful in a description of the baryonic ground states. However it gives no clue about excited states and quarks dynamics inside a particle. Because lattice QCD is still not able to reproduce even ground states masses the hyperons spectrum is calculated using effective theories [ref]. Despite a huge theoretical and experimental effort a theoretical predictions and experimental data are still far away from agreement, especially in high mass range. The example of such is presented in fig. 1.2.

1.2 Form factors

Any kind of a scattering experiment performed to examine physics inside baryons faces a fundamental problem of a rich internal structure of them. An complicated interactions inside the baryon can be treated together and their impact on a scattering could be taken into consideration by one scalar function called a form factor $F(q)$,

$$\frac{d\sigma}{d\Omega} = \left(\frac{d\sigma}{d\Omega} \right)_{point-like} |F(\vec{q})|^2. \quad (1.1)$$

As long as a target is static and spin-less the form factor is a the Fourier Transform of the charge deccity in target,

$$F(\vec{q}) = \int \rho(\vec{x}) e^{i\vec{q}\cdot\vec{x}} d^3x. \quad (1.2)$$

Practically this relation occures whent a target is much heavier than a projectle, like in Rutheford experiment [1]. In case of electron on proton scattering situation is more complicated because both particles has a spin and a proton gets recoil after scattering. A solution for this problem is called the Rosenbluth formula and looks as follows

$$\left. \frac{d\sigma}{d\Omega} \right|_{lab} = \left(\frac{\alpha^2}{4E^2 \sin^4 \frac{\theta}{2}} \right) \frac{E'}{E} \left[\left(F_1(q^2)^2 - \frac{\kappa^2 q^2}{4M^2} F_2(q^2)^2 \right) \cos^2 \frac{\theta}{2} - \frac{q^2}{2M^2} (F_1(q^2) + \kappa F_2(q^2))^2 \sin^2 \frac{\theta}{2} \right], \quad (1.3)$$

where $F_1(q^2)$ and $F_2(q^2)$ are two independent form factors, κ anomalus magnetic moment, q a four-momentum transfer. Factor

$$\frac{E'}{E} = \frac{1}{1 + \frac{2E}{M} \sin^2 \frac{\theta}{2}} \quad (1.4)$$

is conected with the proton recoil. Because functions F_1 and F_2 form an interference term it is convinient to express them as a linear combination of G_e and G_M .

$$G_e = F_1 + \frac{\kappa q^2}{4M^2} F_2 \quad (1.5)$$

$$G_M = F_1 + \kappa F_2 \quad (1.6)$$

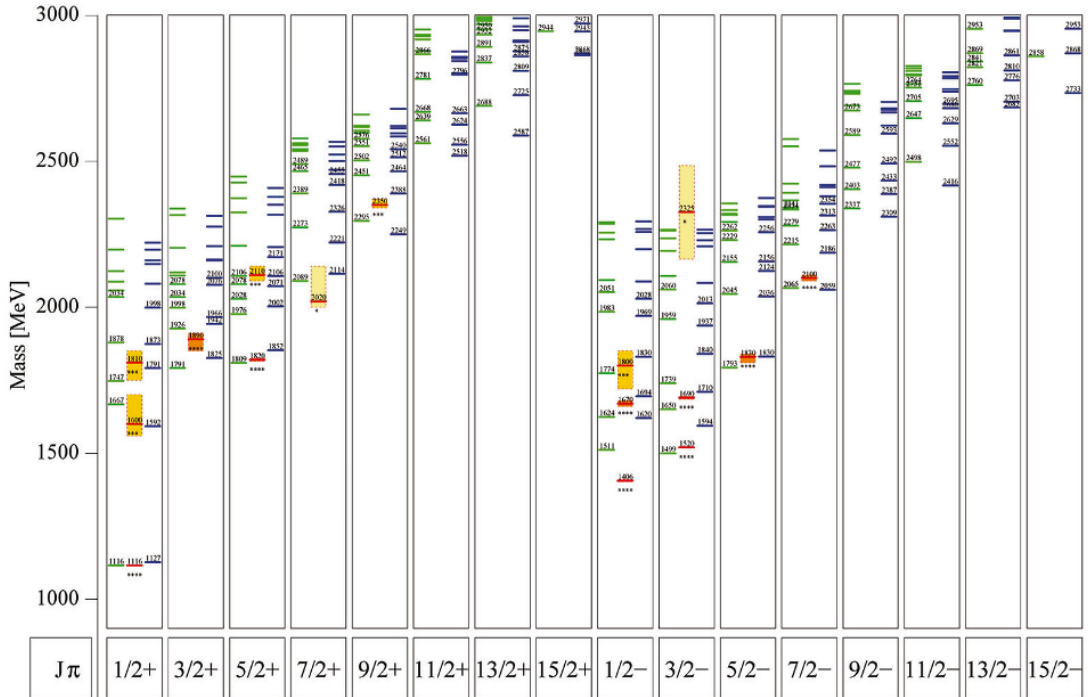


FIGURE 1.2: The comparison of experimental data (middle column) and theoretical predictions (left, and right column) of relativistically covariant constituent quark models for Λ hyperons. The picture shows how limited is our experimental knowledge compare to theroetical predictions. The picture is taken from [7]

1.3 Dalitz decays

The idea of form-factors was introduced first time in context of scattering experiments. A Feynmann diagram for such phenomena is shown in fig. 1.3 a). Due to kinematic constraints for the scattering a four-momentum q^2 is always negative - a projectile transfers part of its four-momentum into target. However an idea of the form factor can be extended to annihilation experiments, where $q^2 > 0$ (fig.1.3 b)). Unfortunately, to produce a baryon-antibaryon pair energy equal at least their masses is required. It means that q^2 can not be smaller than $4M_b^2$. This gap in q^2 can be explored in a range $0 < q^2 < 4M_b^2$ by process called a Dalitz decay.

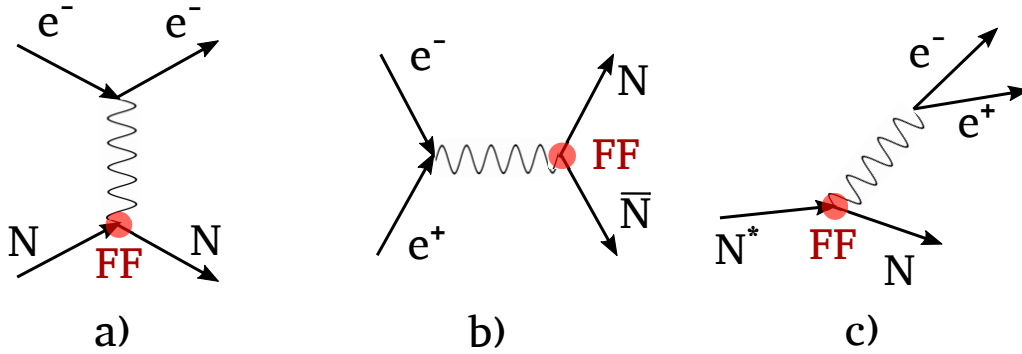


FIGURE 1.3: Three processes involving a nucleon electromagnetic form factors: a) an electron-nucleon scattering, b) an electron-positron annihilation, c) a nucleon Dalitz decay.

The Dalitz decay of a nucleon (is fig.1.3 c)) is a reaction

Chapter 2

The HADES detector

2.1 The HADES upgrades

Chapter 3

Deta analysis

The HADES experiment has performed a proton-proton experiment with beam kinetic energy 3.5 GeV in September 2018. Data collected during this experiment allowed to conduct a series of analysis devoted to hyperons [ref]. In this thesis the next step in hyperon studies is presented. The four particles $p\pi^-\pi^+\pi^-$ final state was analyzed. It allows to reconstruct the inclusive signal of $\Lambda(1520)$ and $\Lambda(1116)K^0$ signal. The obtained results were used to constrain simulation of a new experiment devoted to hyperon studies 5.

All methods developed for pp@3.5 GeV experiment were used for data from pNb@3.5 GeV experiment. A similar analysis ..

3.1 Particles identification

The HADES detector allows for two complementary methods of particles analysis. A first of them bases on particles time of flight measured in the TOF detectors and particle's momentum measured in the MDC. A second method bases on MDC exclusively and uses combined information about particles' momentum and energy losses. The first one is favoured due to better precision, however a limited geometrical of the TOF detectors reduces detection efficiency by a factor 0.8 for each particle. In case of four particles final state, discussed in this thesis, a total loss caused by the TOF detectors can reach 60% of all detected particles. For that reason the $\frac{dE}{dx}$ vs. momentum identification method was used. Cuts were optimized in Munich group involved in HADES experiment and described in [ref].

3.2 Event selection

Among all registered events only these with at least four charged particles (two positive and two negative) has been registered in the HADES. In case of situation when detector registered more particles the combination with the lowest χ^2 was taken. ...

3.3 Reaction kinematics

A next step after an event selection was a look into a missing mass spectrum of all analyzed events. Because the easiest production mechanism for a pp reaction is as follows

$$pp \rightarrow pK^+\Lambda(1116), \quad (3.1)$$

hence, for a $\Lambda(1116)$ decaying into $\Lambda(1520)\pi^+\pi^-$ a final state is

$$pppK^+p\pi^-\pi^+\pi^-. \quad (3.2)$$

The smallest missing mass for observed final state is a sum of p and K^+ mass. At the same time for a main background source: a multipion production in a target, the smallest missing mass is equal a sum of p and π^+ mass. The missing mass spectrum is presented in fig. ??.

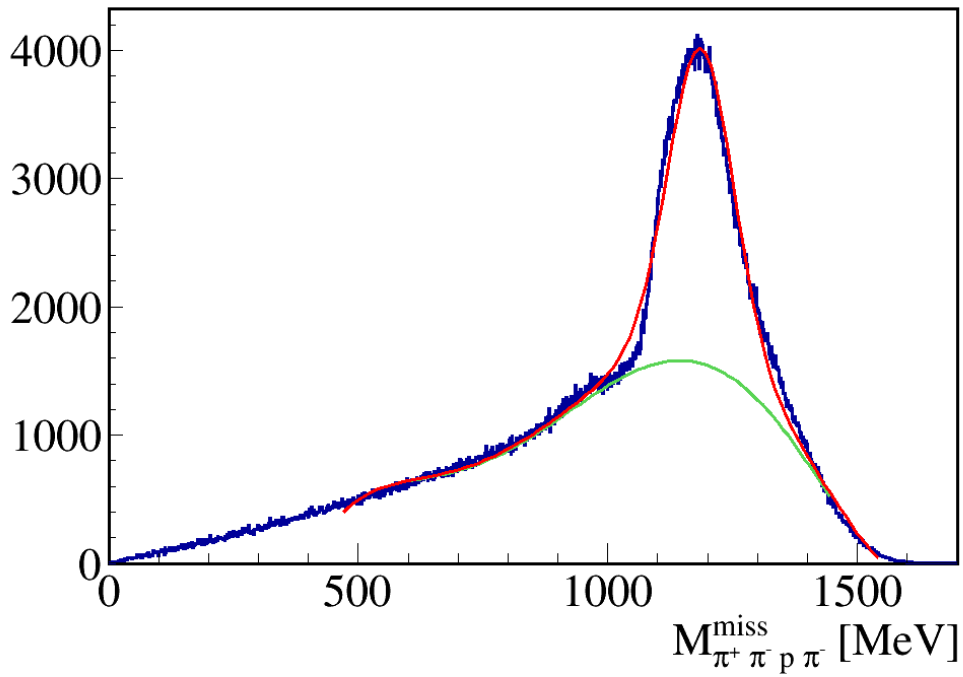


FIGURE 3.1: The missing mass of $p\pi^-\pi^+\pi^-$ system. The resonance behaviour around 1200 MeV is clearly visible. The red line represents sum of signal (a Voigt function) and a background (5-th order polynomial) fit.

3.4 The $\Lambda(1116)$ Reconstruction

3.5 The $\Lambda(1520)$ Reconstruction

3.6 The $\Lambda(1116)K^0$ reconstruction

3.7 results from p Nb experiment

Chapter 4

Neural networks

4.1 Introduction into artificial neural networks

4.2 The ROC curve and the optimal classifier

One of the most common problem in machine learning is a binary classification, when a data set has to be divided into two subsets, fulfilling serian requirements. A simple example of such a problem is distinction between signal and bacground events in deta collected by experiment. We would like to have a function which takes as agruments set of physical observables (eg. particles' energy, momentum, coordinates of vertexes), represents by \vec{x} and returns sigle number. More formally, a clasfyier can be call any function $h : \vec{x} \rightarrow \mathbb{R}$ designed in such a way, that high $h(\vec{x})$ values correspond signal events and low $h(\vec{x})$ values correspond background event. A threshold value $h(\vec{x})=c$, which is the value separating signal and bacground events is called a working point, and has to be set by a user. The signal efficiency will be defined as $\epsilon_S = \int d\vec{x} \rho_S(\vec{x}) \Theta(h(\vec{x}) - c)$ and respectively a background efficiency $\epsilon_B = \int d\vec{x} \rho_B(\vec{x}) \Theta(h(\vec{x}) - c)$.

The problems how to represent a clasfyier performance, how to compare different clasfyiers and how to choose proper working point have been discussed since many years.

4.3 The data-driven approach

The original paper by Metodiev, Nachman and Thaler [8] the others show the idea of a data-driven analysis in details. In this chapter I want to introduce main concepts, necessary to understand how the proposed metode helps in week decays recosntruction.

In a classical approach to supervized machine learning, a model learns its properties usign sets of labeled data. Of course providing good training sets is always a problem. To do this someone can use either experimental data, labeled by a user, or simulation. In first case a user uses his external

knowledge about the data to describe it. In second case the user fully rely on simulation. (opisz zagrożenia)

The data-driven analysis avoids inconveniences of two mentioned methods. It requires neither labeling nor simulation. According to Neyman-Pearson lemma [9] the optimal classifier for two sets, A and B is a function given by a density ratio

$$h_{opt}^{A/B}(\vec{x}) = \frac{\rho_A}{\rho_B} \quad (4.1)$$

or any monotonous function of $\frac{\rho_A}{\rho_B}$. Assuming that both sets A and B contains signal (s) and background (b) events and a statistical distribution of s and b is the same in A and B, we can write (4.1) in the following way

$$h_{opt}^{A/B} = \frac{f_1 \rho_s + (1 - f_1) \rho_b}{f_2 \rho_s + (1 - f_2) \rho_b} = \frac{f_1 \rho_s / \rho_b + 1 - f_1}{f_2 \rho_s / \rho_b + 1 - f_2} = \frac{f_1 h_{opt}^{s/b} + 1 - f_1}{f_2 h_{opt}^{s/b} + 1 - f_2}. \quad (4.2)$$

It can be proven that $\partial_{h_{opt}^{s/b}} h_{opt}^{A/B} > 0$, what means that optimal classifier for both cases is the same. It is important to underline that the reasoning gives no clue about the working points for both cases.

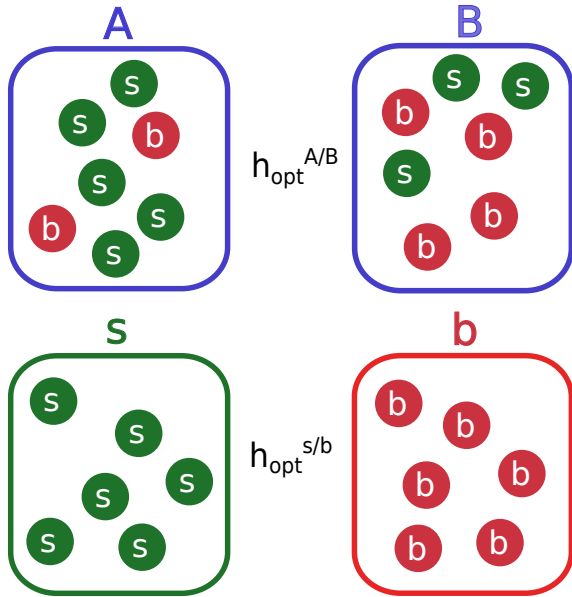


FIGURE 4.1: A data-driven approach visualisation. According to [8] the optimal classifier for sets A and B is equivalent to optimal classifier for sets s and b.

4.4 Application for analysis

In case of $\Lambda(1520)$ reconstruction the data driven approach was used to replace set of geometrical cuts and enhance a $\Lambda(1116)$ signal, so for the neural network all events with $\Lambda(1116)$ were treated as a signal and without like a background. For all events an invariant mas of $p\pi^-$ pair was plotted.

Using this spectrun I have divided the dataset in two subsets: for $M_{p\pi^-}^{inv} \in (1015, 1125)$ and $M_{p\pi^-}^{inv} \notin (1015, 1125)$. In the first of them a ratio between $\Lambda(1116)$ and background is clearly different than in the secon.

Chapter 5

Simulations of a new experiment

The HADES collaboration is one of the leading forces of a FAIR Phase-0 project. Within the scope of FAIR project a $pp@4.5\text{GeV}$ experiment is going to be performed. It gives a great opportunity to measure hyperons' Dalitz decays (see Chapter 1). One of the goals of my work was to carry out a simulation of such an experiment.

5.1 An estimation of cross-sections

In energy range of $1\text{GeV} < \sqrt{S} < 6\text{GeV}$ an inclusive cross section for $\Lambda(1116)$ and $\Sigma(1193)$ were measured for many different energies [10–12]. Also an inclusive cross section for $\Lambda(1405)$ production was measured for two different energies [13, 14], and for $\Lambda(1520)$ is known for one energy [10] in this range. In contrast to the exclusive production cross section, inclusive cross sections for hyperons' production are poorly known. First step to perform a simulation was to estimate possible cross sections based on available knowledge.

5.1.1 $\Lambda(1116)$ inclusive cross section

The first step for all estimations is a parametrization of a $\Lambda(1116)$ inclusive production. In a given energy range there are four measured values. Moreover I made two additional assumptions i) the inclusive cross section is equal 0 for threshold energy, ii) for energy below one pion mass (140MeV) the inclusive and the exclusive cross sections are the same. For the parametrization I can use cross section measured for $pp \rightarrow pK^+\Lambda(1116)$ for \sqrt{S} below ???. To all available data points meeting my requirements I fitted a 3th order polynomial

$$\sigma_{pp \rightarrow \Lambda(1116)X}(\sqrt{S}) = 48 \cdot (\sqrt{S} - 2.55) + 292.6 \cdot (\sqrt{S} - 2.55)^2 - 45.4 \cdot (\sqrt{S} - 2.55)^3. \quad (5.1)$$

Fit result, together with residual plot is shown in 5.1 by a blue dotted line. This parametrization forms the basis for all inclusive cross sections estimated in my work.

5.1.2 $\Sigma(1193)$ inclusive cross section

According to PDG [15] almost all $\Sigma(1193)$ s decay into $\Lambda(1116)$. I means that the inclusive $\Lambda(1116)$ signal contains a fraction deriving from $\Sigma(1193)$ decays. However knowing a relation between $\Lambda(1116)$ and $\Sigma(1193)$ it is possible to disantangle both contributions.

A $\Sigma(1193)/\Lambda(1116)$ ratio was measured by COSY and others [11]. Additionally the COSY collaboration proposed a parametrization of the ratio for eccess energy $\epsilon < 200MeV$. Above this energy ($\epsilon > 200MeV$) a linear parametziation

$$\frac{\Lambda(1116)}{\Sigma(1193)}(\epsilon) = 2.215 - 2.7 \cdot 10^{-5}\epsilon \quad (5.2)$$

describes data quite well ($\chi^2 = 0.89$). In fact for $\epsilon > 200MeV$ the ratio is almost constant and does not depend on energy.

Knowing the $\Lambda(1116)/\Sigma(1193)$ I was able to disantagle a $\Lambda(1116)$ and $\Sigma(1193)$ production. Using determinated ratio and the $\Lambda(1116)$ production (let me call it P_1) parametrization given by eq. 5.1(called P_2) I created following set of equations,

$$P_1(\epsilon) = \frac{L(\epsilon)}{S(\epsilon)} = \frac{L(\sqrt{S} - \Lambda(1116)_{thr})}{S(\sqrt{S} - \Sigma(1193)_{thr})} = P_1(\sqrt{S}), \quad (5.3)$$

$$P_2(\sqrt{S}) = \Lambda(\sqrt{S}) + \Sigma(\sqrt{S}), \quad (5.4)$$

Where Σ represents the inclusive $\Sigma(1193)$ production cross section and Λ the Lz cross section accordingly. Solving the first equation and shifting an argument by $\Sigma(1385)_{thr}$ I obtained an equation,

$$\Sigma(\sqrt{S}) \cdot P_1(\sqrt{S} + \Sigma(1193)_{thr}) = \Lambda(\sqrt{S} - \Lambda(1116)_{thr} + \Sigma(1193)_{thr}). \quad (5.5)$$

Now, using eq. 5.5 and 5.4 I got a recurrence relation

$$\Lambda(\sqrt{S} - \Lambda(1116)_{thr} + \Sigma(1193)_{thr}) = P_1(\sqrt{S} + \Sigma(1193)_{thr}) \left(P_2(\sqrt{S}) - \Lambda(Sqs) \right). \quad (5.6)$$

Assuming that $\Lambda(\Lambda(1116)_{thr}) = 0$ and $\Sigma(\Sigma(1193)_{thr}) = 0$, the above equation can be solved with any given precision. For the purpose of cross sections estimation a single step was set $\Delta M = \frac{\Sigma(1193)_{thr} - \Lambda(1116)_{thr}}{10}$, obtained decomposition is shown in 5.1 by dashed lines. A characteristic “kick” on the green line corresponds to energy when two parametrizations of $\frac{\Lambda(1116)}{\Sigma(1193)}$ ratio are glued (see fig ??).

5.1.3 $\Lambda(1520)$, $\Lambda(1405)$ and $\Sigma(1385)$ production cross sections

A knowledge about cross sections for Λ and Σ in function of \sqrt{S} or energy over the freshold ϵ gives a possibility to estimate cross section for excided hyperon states. As a first approximation I

have assumed that a production matrix element for ground and excited states is the same. It means that only factor cases the difference in cross section is available energy over the threshold. It can be expressed by an equation

$$\sigma_{\Lambda^*X}(\Lambda_{thr}^* + \epsilon) = \sigma_{\Lambda X}(\Lambda_{thr} + \epsilon), \quad (5.7)$$

or in terms of \sqrt{S}

$$\sigma_{\Lambda^*X}(\sqrt{S}) = \sigma_{\Lambda X}(\sqrt{S} - \Lambda_{thr}^* + \Lambda_{thr}). \quad (5.8)$$

Using the equation 5.7 I have calculated expected cross sections for the excited hyperons states $\Lambda(1520)$ and $\Sigma(1385)$. They are shown in 5.1 as blue and green star.

A $\Lambda(1405)$ exclusive cross section was measured for two different energies by HADES [13] and COSY-tof [14] experiment. In [13] authors proposed a phenomenological parametrization of $\Lambda(1405)$ exclusive cross section ,

$$\sigma_{\Lambda(1405)pK^+}^{excl}(\epsilon) = \frac{1}{3} \sigma_{\Lambda(1116)pK^+}^{excl}(\epsilon). \quad (5.9)$$

I have followed the same relation for inclusive reactions multiplying the inclusive $\Lambda(1116)$ cross section by factor 1/3. Result is shown in 5.1 by a magenta line. A magenta star shows point corresponding to $E_k = 4.5\text{GeV}$ proton beam. Numerical values of the estimated cross sections are in tab. 5.1.

5.1.4 $\Xi^-(1322)$

Knowledge about a double-strange hyperon $\Xi^-(1322)$ is extremely limited.

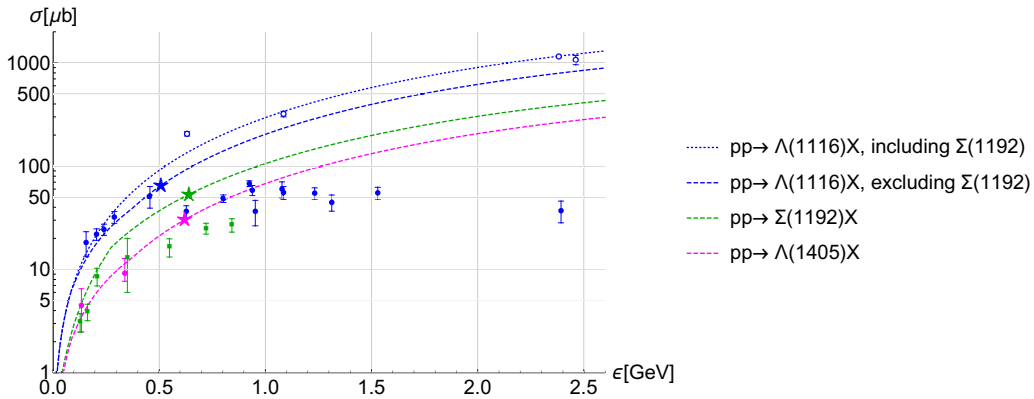


FIGURE 5.1: An estimated cross sections for Hyperons production. Blue dotted line shows an inclusive $\Lambda(1116)$ production. It was decomposed into two components: i) $\Lambda(1116)$ - blue dashed line and ii) $\Sigma(1192)$ green dashed line. Magenta dashed line represents a parametrization of $\Lambda(1405)$ cross section. All points refer to experimental data measured by different experiments [10–14]. Color code is the same like for lines. Full points represent an exclusive cross section, empty points an inclusive one.

5.2 Decay branching ratios

Because Dalitz decays of hyperons were never measured a decay branching ratio have to be estimated considering available data. A first approximation may be obtained using result for a non-strange sector. For a reaction $\Delta^+ \rightarrow p e^+ e^-$ the HADES reported [16] $BR_{\Delta \rightarrow p e^+ e^-} = (4.19 \pm 0.62 \text{ syst.} \pm 0.34 \text{ stat.}) \times 10^{-5}$. More precise estimation bases on, measured by CLAS collaboration [17], hyperons' radiative decays. A relation between radiative decays and Dalitz decays is given by the formula derived in F. Scozzi PhD thesis [18],

$$\Gamma^{N^* \rightarrow N e^+ e^-} = 1.35 \cdot \alpha \Gamma^{N^* \rightarrow N \gamma}. \quad (5.10)$$

For $\Lambda(1520)$ and $\Sigma(1385)$ decay with for real photon decay are known. For Lss the branching ratio have to be estimated using other decay channels [ref]. Obtained results (tab. 5.1) are located in range of measured BR for Δ^+ dalitz decay.

5.3 Background channels selection

To obtain a reliable simulation a cocktail of background channels should be considered and tested. In case of hadronic physic, for low and medium energies, due to lack of approximation theorem, get a realistic background is a very challenging task. For a $\sqrt{S} = 3.46$ GeV a hadronic matter tends to form resonances. It means that almost all hadrons in final states originate from decays of high-mass resonances. Because knowledge about properties of such a resonances is limited I made a simplified assumption that all pions are produced directly, without any intermediate state and with angular distribution defined just by a reaction phase-space. List of all background channels considered during studies is presented in tab. 5.1.

All channels considered as a $\Xi^-(1322)$ background have to consist $p \pi^- \pi^-$ in final state. A dominant one is a multi-pion production, however thanks to topological cuts (see chapter 5.4.3) this kind of the background is relatively easy to filter out. Second kind of the background considered in simulation is a $\Lambda(1116)$ production associated with π^- . Reactions much more challenging because the $\Lambda(1116)$ decay vertex is displaced from a target, the same like in signal reaction. Cross sections for channels number 2-7 are taken from [12]. When data in a proper energy range is missing, the value for the lowest available energy above $\sqrt{S} = 3.46$ GeV is taken. that conservative assumption gives me a safe margin.

For all channels consisting of the hyperons' Dalitz decays a final state is the same: $p \pi^- e^+ e^-$. That allows me to use the same background cocktail for all three channels. I divided possible background sources into three main groups. Firstly I considered a multi-pion production in a target area, channels: 14, 16 and 18. A di-lepton pair originates from a π^0 Dalitz decay and combination of p and π^- creates false $\Lambda(1116)$ signal. These channels differ from signal one mainly by a decay geometry. The $\Lambda(1116)$ decays via weak interaction with long lifetime $c\tau = 7.89$ cm [15], so its decay vertex is expected to be observed outside the target. A second group, channels 19, 21, 23,

TABLE 5.1: List of signal (S) and background (B) channels for simulated reactions. Each channel containing Δ Dalitz decay is listed below reference channel, used for cross section estimation.

no.	Channel	$\sigma [\mu\text{b}]$	Type
$\Xi^-(1322)$ production			
1	$pK^+K^+\Xi^-(1322)$	3.6/0.35	S
2	$pp\pi^+\pi^+\pi^-\pi^-$	227	B
3	$p\Lambda(1116)K_S^0\pi^+$	30	B
4	$p\Lambda(1116)K^+\pi^+\pi^-$	21	B
5	$n\Lambda(1116)K_S^0\pi^+\pi^+$	10	B
6	$p\Sigma(1193)K_S^0\pi^+$	9	B
7	$ppK_S^0K_S^0$	1.6	B
Dalitz decays of hyperons			
8	$pK^+\Lambda(1520)[\Lambda(1116)e^+e^-]$	69.6, BR = 8.4×10^{-5}	S
9	$pK^+\Lambda(1405)[\Lambda(1116)e^+e^-]$	32.2, BR = 5.3×10^{-6}	S
10	$pK^+\Sigma(1385)[\Lambda(1116)e^+e^-]$	56.24, BR = 1.1×10^{-4}	S
11	$pK^+\Lambda(1520)[X]$	69.6	B
12	$pK^+\Lambda(1405)[X]$	32.2	B
13	$pK^+\Sigma(1385)[X]$	56.24	B
14	$pp\pi^+\pi^-\pi^0$	1840	B
15	$p\pi^+\pi^-\Delta^+[pe^+e^-]$	2760, BR = 4.5×10^{-5}	B
16	$pn\pi^+\pi^+\pi^-\pi^0$	300	B
17	$p\pi^+\pi^+\pi^-\Delta^0[ne^+e^-]$	450, BR = 4.5×10^{-5}	B
18	$pp\pi^+\pi^-\pi^0\pi^0$	300	B
19	$p\Lambda(1116)K^+\pi^0$	43	B
20	$K^+\Lambda(1116)\Delta^+[pe^+e^-]$	64, BR = 4.5×10^{-5}	B
21	$n\Lambda(1116)K^+\pi^+\pi^0$	20	B
22	$\pi^+K^+\Lambda(1116)\Delta^0[ne^+e^-]$	30, BR = 4.5×10^{-5}	B
23	$p\Lambda(1116)K^+\pi^0\pi^0$	10	B
24	$p\Sigma(1193)K_S^0\pi^+$	9	B
25	$p\Lambda(1116)K^+\pi^0\pi^0\pi^0$	7	B

24, 25, contains $\Lambda(1116)$ production associated with a di-lepton source. In this case I have a real $\Lambda(1116)$ and a e^+e^- pair coming from decay of different particles, mainly π^0 . The cross section are taken from [12]. The third source of background are Dalitz decays of non-strange baryons associated with $\Lambda(1116)$ production. The braching ratio was mesured only for Δ^+ Dalitz [16], for Δ^0 Dalitz I have assumed the same value. A production cross section for the channels containing Δ has been calculated assumed that all pions comes from the reosnacnes decays. For example, channel 14 is the final state for reaction $pp \rightarrow p\Delta^+[p\pi^0]\pi^+\pi^-$. Assuming that the Δ decay into pions conserv an izospin symmetry I used Clebsch-Gordan coefficients to calculate a ratio

$$\frac{\Delta^+ \rightarrow p\pi^0}{\Delta^+ \rightarrow n\pi^+} = \frac{2}{1}. \quad (5.11)$$

Hence, a total cross section for the reaction $pp \rightarrow p\Delta^+\pi^+\pi^-$ is $\frac{3}{2} \cdot \sigma_{pp \rightarrow pp\pi^+\pi^-\pi^0}$. The cross sections for other channels containing Δ dalitz decay were calculated in a similar way. Each Δ channel is listed below a reference multi-pion production channel.

5.4 Simulations results

The simulation has been performed using following frameworks. The PLUTO event generator [19, 20] to simulate reactions in the target, the GEANT3 [21] software to simulate particles propagation through the detector and to simulate decay of unstable reaction's products like $\Lambda(1116)$ or K_S^0 . After all physics simulations, the detector answer and a full reconstruction chain was done in the HYDRA framework. All together gives me a realistic simulation of an examined physics, and the HADES behaviour. The new HADES upgrades: new RICH, and the FwDet (see chapter 2.1) were included.

5.4.1 Particles identification

The particle identifications algorithms used for simulation are, in principle, the same as for data collected during experiment. In first step all particle candidates are filtered to find events in which track reconstructed in the MDC is fitted with the RICH rings. Additionally a Time-Of-Flight and Beta for leptonic track has to lay within a graphical cut. If both criteria were fulfilled they are treated as lepton candidates. In next step for all non-leptonic candidates the mass is calculated according to the formula

$$m = \frac{pc}{\beta\gamma}. \quad (5.12)$$

For protons and pions the mass cuts are 650-1127 MeV and 40-240 MeV respectively.

5.4.2 Hyperons Dalitz decays

5.4.3 Cascade decay

Chapter 6

Conclusions

Bibliography

- [1] H. Geiger, “On the scattering of α -particles by matter,” *Proceedings of the Royal Society of London A* **81** (Jul, 1908) 174–177.
- [2] S. Chatrchyan, V. Khachatryan, A. M. Sirunyan, A. Tumasyan, W. Adam, and et. al. [CMS Collaboration], “Observation of a new boson at a mass of 125 GeV with the CMS experiment at the LHC,” *Physics Letters B* **716** no. 1, (Sept., 2012) 30–61, [arXiv:1207.7235](https://arxiv.org/abs/1207.7235) [hep-ex].
- [3] G. Aad, T. Abajyan, B. Abbott, J. Abdallah, S. Khalek, A. Abdelalim, O. Abdinov, R. Aben, M. Abolins, O. Abouzeid, H. Abramowicz, H. Abreu, B. Acharya, L. Adamczyk, D. Adams, T. Addy, J. Adelman, S. Adomeit, and L. Zwalinsk, “Observation of a new particle in the search for the standard model higgs boson with the atlas detector at the lhc,” *Physics Letters B* **716** (09, 2012) 1–29.
- [4] M. Gell-Mann, “A schematic model of baryons and mesons,” *Physics Letters* **8** (Feb, 1964) 214–215.
- [5] G. Zweig, “An $su(3)$ model for strong interaction symmetry and its breaking,” *CERN Report* **8182/TH.401** (Jen, 1964) .
- [6] V. E. Barnes, P. L. Connolly, D. J. Crennell, B. B. Culwick, W. C. Delaney, W. B. Fowler, P. E. Hagerty, E. L. Hart, N. Horwitz, P. V. C. Hough, J. E. Jensen, J. K. Kopp, K. W. Lai, J. Leitner, J. L. Lloyd, G. W. London, T. W. Morris, Y. Oren, R. B. Palmer, A. G. Prodell, D. Radojićić, D. C. Rahm, C. R. Richardson, N. P. Samios, J. R. Sanford, R. P. Shutt, J. R. Smith, D. L. Stonehill, R. C. Strand, A. M. Thorndike, M. S. Webster, W. J. Willis, and S. S. Yamamoto, “Observation of a hyperon with strangeness minus three,” *Phys. Rev. Lett.* **12** (Feb, 1964) 204–206.
<https://link.aps.org/doi/10.1103/PhysRevLett.12.204>.
- [7] M. Ronniger and B. Metsch, “Effects of a spin-flavour dependent interaction on light-flavoured baryon helicity amplitudes,” *The European Physical Journal A* **49** (07, 2012) .
- [8] E. M. Metodiev, B. Nachman, and J. Thaler, “Classification without labels: learning from mixed samples in high energy physics,” *Journal of High Energy Physics* **2017** no. 10, (Oct, 2017) . [http://dx.doi.org/10.1007/JHEP10\(2017\)174](http://dx.doi.org/10.1007/JHEP10(2017)174).
- [9] J. Neyman and E. S. Pearson, “On the problem of the most efficient tests of statistical hypotheses,” *Philosophical Transactions of the Royal Society of London* **231** (Feb, 1933) .
<https://doi.org/10.1098/rsta.1933.0009>.

- [10] J. Adamczewski-Musch, G. Agakishiev, O. Arnold, E. T. Atomssa, C. Behnke, J. C. Berger-Chen, J. Biernat, A. Blanco, C. Blume, M. Böhmer, P. Bordalo, S. Chernenko, C. Deveaux, J. Dreyer, A. Dybczak, E. Eppe, L. Fabbietti, O. Fateev, P. Fonte, C. Franco, J. Friese, I. Fröhlich, T. Galatyuk, J. A. Garzón, K. Gill, M. Golubeva, F. Guber, M. Gumberidze, S. Harabasz, T. Hennino, S. Hlavac, C. Höhne, R. Holzmann, A. Ierusalimov, A. Ivashkin, M. Jurkovic, B. Kämpfer, T. Karavicheva, B. Kardan, I. Koenig, W. Koenig, B. W. Kolb, G. Korcyl, G. Kornakov, R. Kotte, A. Krása, E. Krebs, H. Kuc, A. Kugler, T. Kunz, A. Kurepin, A. Kurilkin, P. Kurilkin, V. Ladygin, R. Lalik, K. Lapidus, A. Lebedev, L. Lopes, M. Lorenz, T. Mahmoud, L. Maier, S. Maurus, A. Mangiarotti, J. Markert, V. Metag, J. Michel, S. Morozov, C. Müntz, R. Münzer, L. Naumann, M. Palka, Y. Parpottas, V. Pechenov, O. Pechenova, V. Petousis, J. Pietraszko, W. Przygoda, S. Ramos, B. Ramstein, L. Rehnisch, A. Reshetin, A. Rost, A. Rustamov, A. Sadovsky, P. Salabura, T. Scheib, K. Schmidt-Sommerfeld, H. Schuldes, P. Sellheim, J. Siebenson, L. Silva, Y. G. Sobolev, S. Spataro, H. Ströbele, J. Stroth, P. Strzempek, C. Sturm, O. Svoboda, A. Tarantola, K. Teilab, P. Tlusty, M. Traxler, H. Tsertos, T. Vasiliev, V. Wagner, C. Wendisch, J. Wirth, Y. Zanevsky, and P. Zumbach [HADES Collaboration], “Inclusive Λ production in proton-proton collisions at 3.5 gev,” *Phys. Rev. C* **95** (Jan, 2017) 015207.
<https://link.aps.org/doi/10.1103/PhysRevC.95.015207>.
- [11] T. COSY-TOF Collaboration, M. Abdel-Bary, S. Abdel-Samad, K.-T. Brinkmann, H. Clement, J. Dietrich, E. Doroshkevich, S. Dshemuchadse, K. Ehrhardt, A. Erhardt, W. Eyrich, D. Filges, A. Filippi, H. Freiesleben, M. Fritsch, W. Gast, J. Georgi, A. Gillitzer, J. Gottwald, and P. Żuprański, “Production of λ^0 and σ^0 hyperons in proton-proton collisions,” *European Physical Journal A* **46** (10, 2010) 27–44.
- [12] G. Höhler, “Landolt-börnstein - group i elementary particles, nuclei and atoms,” 7–8. 01, 1983.
- [13] G. Agakishiev *et al.* [HADES Collaboration], “Baryonic resonances close to the $\bar{K}N$ threshold: the case of $\Lambda(1405)$ in pp collisions,” *Phys. Rev. C* **87** (2013) 025201, [arXiv:1208.0205 \[nucl-ex\]](https://arxiv.org/abs/1208.0205).
- [14] I. Zychor, M. Büscher, M. B. A. C, I. Keshelashvili, A. Khoukaz, V. F. V. G, Y. H, T. E, S. G, R. B, H. B, Y. Valda, and C. I, “Lineshape of the $\lambda(1405)$ hyperon measured through its $\sigma^0 \pi^0$ decay,” *Physics Letters B* **660** (02, 2008) 167–171.
- [15] M. Tanabashi, P. Grp, K. Hagiwara, K. Hikasa, K. Nakamura, Y. Sumino, F. Takahashi, J. Tanaka, K. Agashe, G. Aielli, C. Amsler, M. Antonelli, D. Asner, H. Baer, S. Banerjee, R. Barnett, T. Basaglia, C. Bauer, and J. Beatty, “Review of particle physics: Particle data group,” *Physical Review D* **98** (08, 2018) .
- [16] J. Adamczewski-Musch, O. Arnold, E. T. Atomssa, C. Behnke, A. Belounnas, A. Belyaev, J. C. Berger-Chen, J. Biernat, A. Blanco, C. Blume, M. Böhmer, P. Bordalo, S. Chernenko, L. Chlad, C. Deveaux, J. Dreyer, A. Dybczak, E. Eppe, L. Fabbietti, O. Fateev, P. Filip, P. Finocchiaro, P. Fonte, C. Franco, J. Friese, I. Fröhlich, T. Galatyuk, J. A. Garzón, R. Gernhäuser, M. Golubeva, F. Guber, M. Gumberidze, S. Harabasz, T. Heinz, T. Hennino, S. Hlavac, C. Höhne, R. Holzmann, A. Ierusalimov, A. Ivashkin, B. Kämpfer,

- T. Karavicheva, B. Kardan, I. Koenig, W. Koenig, B. W. Kolb, G. Korcyl, G. Kornakov, R. Kotte, W. Kühn, A. Kugler, T. Kunz, A. Kurepin, A. Kurilkin, P. Kurilkin, V. Ladygin, R. Lalik, K. Lapidus, A. Lebedev, T. Liu, L. Lopes, M. Lorenz, T. Mahmoud, L. Maier, A. Mangiarotti, J. Markert, S. Maurus, V. Metag, J. Michel, E. Morinière, D. M. Mihaylov, S. Morozov, C. Müntz, R. Münzer, L. Naumann, K. Nowakowski, M. Palka, Y. Parpottas, V. Pechenov, O. Pechenova, V. Petousis, O. Petukhov, J. Pietraszko, W. Przygoda, S. Ramos, B. Ramstein, A. Reshetin, P. Rodriguez-Ramos, P. Rosier, A. Rost, A. Sadovsky, P. Salabura, T. Scheib, H. Schuldes, E. Schwab, F. Scozzi, F. Seck, P. Sellheim, J. Siebenson, L. Silva, Y. G. Sobolev, S. Spataro, H. Ströbele, J. Stroth, P. Strzempek, C. Sturm, O. Svoboda, P. Tlusty, M. Traxler, H. Tsertos, E. Usenko, V. Wagner, C. Wendisch, M. G. Wiebusch, J. Wirth, Y. Zanevsky, P. Zumbbruch, and A. V. Sarantsev [HADES Collaboration Collaboration], “ $\Delta(1232)$ Dalitz decay in proton-proton collisions at $T = 1.25$ GeV measured with HADES at GSI,” *Phys. Rev. C* **95** (6, 2017) 065205. <https://link.aps.org/doi/10.1103/PhysRevC.95.065205>.
- [17] S. Taylor, G. S. Mutchler, G. Adams, P. Ambrozewicz, E. Anciant, M. Anghinolfi, B. Asavapibhop, G. Asryan, G. Audit, H. Avakian, H. Bagdasaryan, J. P. Ball, S. Barrow, V. Batourine, M. Battaglieri, K. Beard, M. Bektasoglu, M. Bellis, N. Benmouna, B. L. Berman, N. Bianchi, A. S. Biselli, S. Boiarinov, B. E. Bonner, S. Bouchigny, R. Bradford, D. Branford, W. J. Briscoe, W. K. Brooks, S. Bültmann, V. D. Burkert, C. Butuceanu, J. R. Calarco, D. S. Carman, B. Carnahan, S. Chen, P. L. Cole, D. Cords, P. Corvisiero, D. Crabb, H. Crannell, J. P. Cummings, E. D. Sanctis, R. DeVita, P. V. Degtyarenko, H. Denizli, L. Dennis, A. Deur, K. V. Dharmawardane, C. Djalali, G. E. Dodge, D. Doughty, P. Dragovitsch, M. Dugger, S. Dytman, O. P. Dzyubak, H. Egiyan, K. S. Egiyan, L. Elouadrhiri, A. Empl, P. Eugenio, R. Fatemi, G. Feldman, R. G. Fersch, R. J. Feuerbach, T. A. Forest, H. Funsten, M. Garçon, G. Gavalian, G. P. Gilfoyle, K. L. Giovanetti, E. Golovatch, C. I. O. Gordon, R. W. Gothe, K. A. Griffioen, M. Guidal, M. Guillo, N. Guler, L. Guo, V. Gyurjyan, C. Hadjidakis, R. S. Hakobyan, J. Hardie, D. Heddle, F. W. Hersman, K. Hicks, I. Hleiqawi, M. Holtrop, J. Hu, M. Huertas, C. E. Hyde-Wright, Y. Ilieva, D. G. Ireland, M. M. Ito, D. Jenkins, K. Joo, H. G. Juengst, J. D. Kellie, M. Khandaker, K. Y. Kim, K. Kim, W. Kim, A. Klein, F. J. Klein, A. V. Klimenko, M. Klusman, M. Kossov, V. Koubarovski, L. H. Kramer, S. E. Kuhn, J. Kuhn, J. Lachniet, J. M. Laget, J. Langheinrich, D. Lawrence, T. Lee, J. Li, A. C. S. Lima, K. Livingston, K. Lukashin, J. J. Manak, C. Marchand, S. McAleer, J. W. C. McNabb, B. A. Mecking, J. J. Melone, M. D. Mestayer, C. A. Meyer, K. Mikhailov, M. Mirazita, R. Miskimen, V. Mokeev, L. Morand, S. A. Morrow, V. Muccifora, J. Mueller, J. Napolitano, R. Nasseripour, S. Niccolai, G. Niculescu, I. Niculescu, B. B. Niczyporuk, R. A. Niyazov, M. Nozar, G. V. O’Rielly, M. Osipenko, A. I. Ostrovidov, K. Park, E. Pasyuk, S. A. Philips, N. Pivnyuk, D. Pocanic, O. Pogorelko, E. Polli, S. Pozdniakov, B. M. Preedom, J. W. Price, Y. Prok, D. Protopopescu, L. M. Qin, B. S. Raue, G. Riccardi, G. Ricco, M. Ripani, B. G. Ritchie, F. Ronchetti, G. Rosner, P. Rossi, D. Rowntree, P. D. Rubin, F. Sabatié, C. Salgado, J. P. Santoro, V. Sapunen, R. A. Schumacher, V. S. Serov, A. Shafi, Y. G. Sharabian, J. Shaw, S. Simionatto, A. V. Skabelin, E. S. Smith, L. C. Smith, D. I. Sober, M. Spraker, A. Stavinsky, S. Stepanyan, S. S. Stepanyan, B. E. Stokes, P. Stoler, I. I. Strakovsky, S. Strauch, R. Suleiman, M. Taiuti, D. J. Tedeschi, U. Thoma, R. Thompson, A. Tkabladze, L. Todor, C. Tur, M. Ungaro, M. F. Vineyard, A. V. Vlassov, K. Wang, L. B. Weinstein,

- H. Weller, D. P. Weygand, C. S. Whisnant, M. Williams, E. Wolin, M. H. Wood, A. Yegneswaran, J. Yun, and L. Zana [CLAS Collaboration Collaboration], “Radiative decays of the $\Sigma^0(1385)$ and $\Lambda(1520)$ hyperons,” *Phys. Rev.* **C71** (5, 2005) 054609.
<https://link.aps.org/doi/10.1103/PhysRevC.71.054609>.
- [18] S. Federico, “Studying excited states of the nucleon with the hades detector at gsi,” PhD thesis, Technische Universitat Darmstadt, Darmstadt (Dec., 2018) .
- [19] I. Fröhlich *et al.*, “Pluto: A Monte Carlo Simulation Tool for Hadronic Physics,” *PoS ACAT* (2007) 076, [arXiv:0708.2382](https://arxiv.org/abs/0708.2382) [nucl-ex].
- [20] I. Frohlich *et al.*, “A versatile method for simulating $pp \rightarrow pp e^+ e^-$ and $dp \rightarrow pn e^+ e^-$ p(spec) reactions,” *Eur. Phys. J. A* **45** (2010) 401–411, [arXiv:0909.5373](https://arxiv.org/abs/0909.5373) [nucl-ex].
- [21] R. Brun, F. Bruyant, M. Maire, A. McPherson, and P. Zancarini, “GEANT3,”.